

Motivation

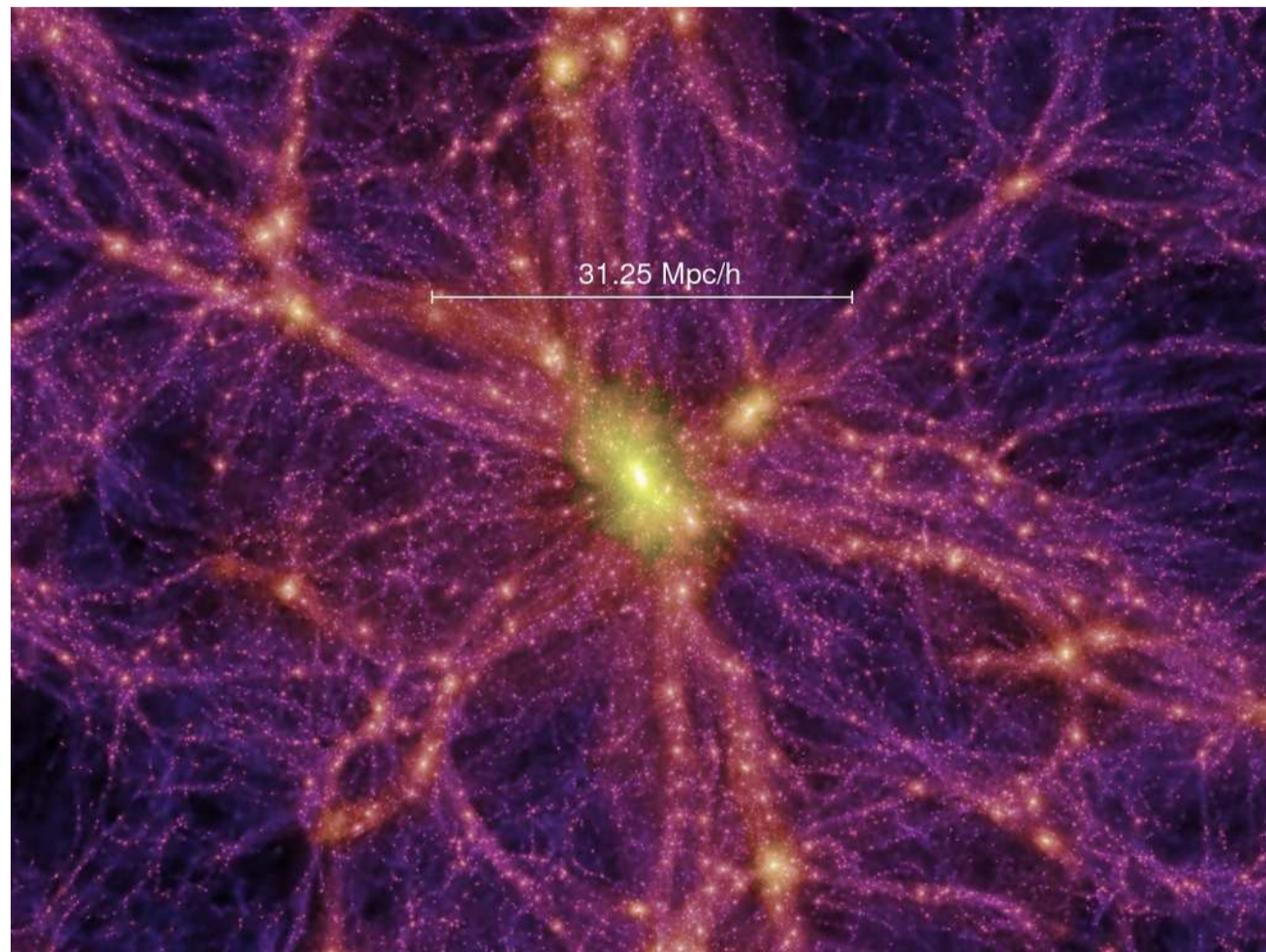


FIGURE 1: Distribution of Dark Matter at $z = 0$ according to the Millennium Run simulation (source: V. Springel et al. '05)

Short History of Structure Formation in the Universe:

- initially small and smooth primordial density perturbations are amplified through gravitational instability and form Large Scale Structure (LSS)
- primordial fluctuations were distributed according to homogeneous Gaussian random processes
- for Gaussian random fields all statistical information is encoded in the power spectrum!
- during most of the evolution inhomogeneities can be treated as linear perturbations (as for the CMB analysis)
- but: as perturbations grow and become non-linear, different modes of the density field become coupled
- this leads to non-Gaussian signatures in the matter density field
- since weak lensing probes low redshift regime and intermediate scales Non-Gaussianities must be taken into account!

Why do we consider the Covariance?

Covariance of statistical quantity x is defined as:

$$C(x_i, x_j) \equiv \langle (x_i - \bar{x}_i)(x_j - \bar{x}_j) \rangle, \quad (1)$$

where $\langle \cdot \rangle$ denotes the ensemble average of x .

- gives error on the quantity x (diagonal elements) and amount of correlation between the different x_i (off-diagonal elements)
- generates in case of the convergence power spectrum $P_\kappa(l)$ non-linear, higher-order correlations
- is essential for the likelihood and Fisher matrix analysis of cosmological parameter estimation
- better understanding important since Gaussian assumption is used often to estimate covariances

Covariance Matrix for Weak Lensing

$$C(l_i, l_j) = \frac{1}{A} \left[\frac{(2\pi)^2}{A_s(l_i)} 2P_\kappa(l_i)\delta_{ij} + T_\kappa(l_i, l_j) \right] \quad (2)$$

where A is the survey volume and $A_s(l_i)$ the shell area. The covariance is decomposed into a **Gaussian** and a **non-Gaussian** part. $P_\kappa(l_i)$ and $T_\kappa(l_i, l_j)$ are the convergence power- and trispectrum defined as:

$$P_\kappa(l) = \int dw \frac{W^2(w)}{d_A^2(w)} P\left(\frac{l}{d_A}, w\right), \quad (3)$$

$$T_\kappa(l_i, l_j) \equiv \int \frac{d^2 l_1}{A_s(l_i)} \int \frac{d^2 l_2}{A_s(l_j)} T_\kappa(\mathbf{l}_1, -\mathbf{l}_1, \mathbf{l}_2, -\mathbf{l}_2), \quad (4)$$

where the weight function $W(w)$ sets the geometry of the background sources (see [1, 3, 6] for more details).

The Halo Model (HM)

Motivation:

- need to model non-linear, higher-order correlation functions
- Perturbation Theory description of gravitational clustering breaks down around $l \simeq 100$
- N-Body simulations of LSS are **computationally very costly**
- HM provides **simple description** for semi-analytic computation of the power- and trispectrum (see Cooray & Sheth [4] for more details)

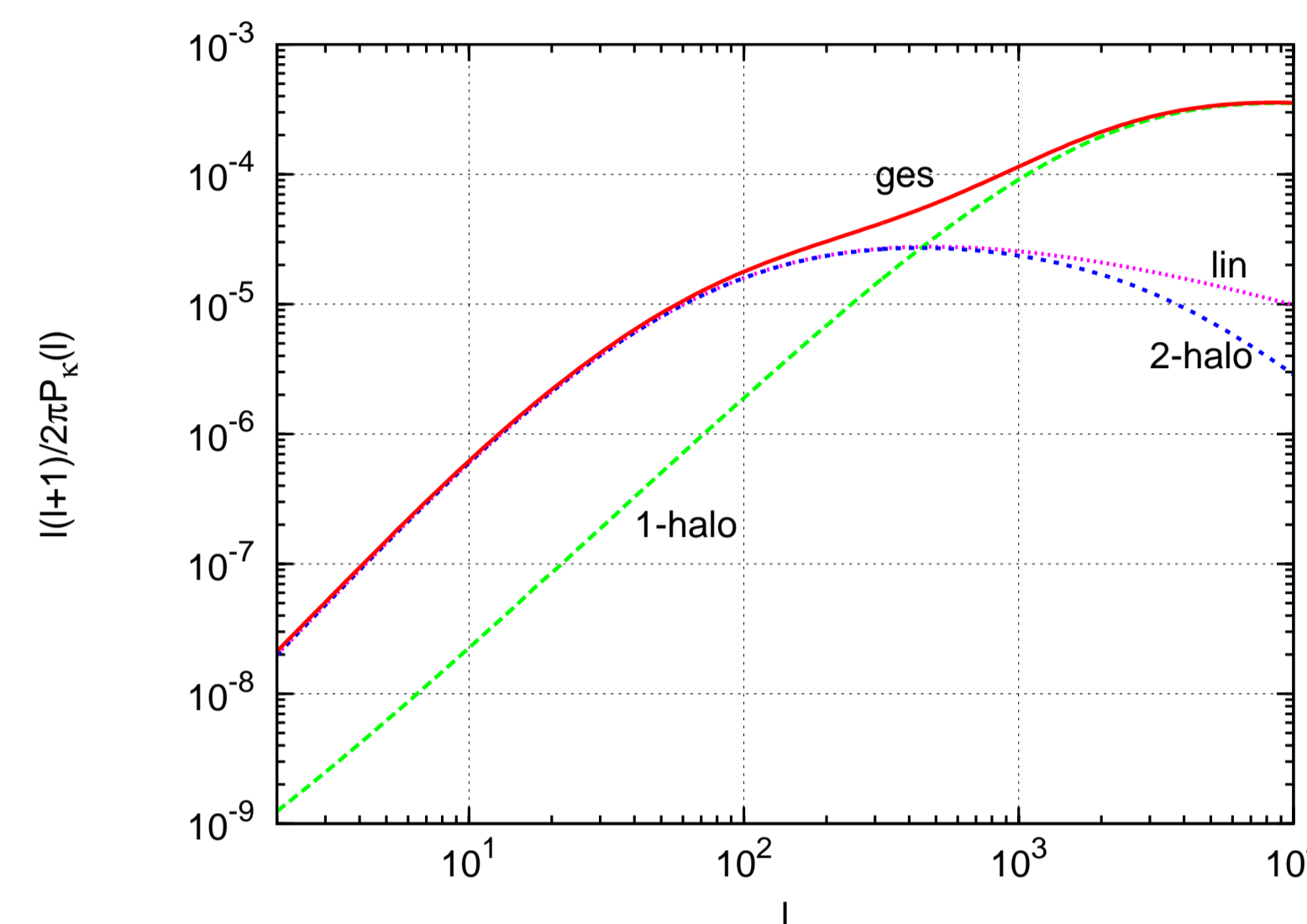


FIGURE 2: The convergence Power Spectrum $P_\kappa(l)$ as generated with the HM. Perturbation theory breaks down around $l \simeq 100$. The Power Spectrum splits into two regimes: The 1-halo term which is dominant on small scales and the 2-halo term which is due to the spatial distribution of halos on large scales.

Ingredients:

- general idea: Dark Matter is distributed in spherically symmetric halos
- physics is split into **two regimes**:
 - **small scales**: spherical collapse model \rightarrow halo profile
 - **large scales**: Perturbation Theory \rightarrow spatial distribution of halos
- halo abundance (Sheth and Tormen mass function)
- halo clustering (Peak-Background-Split \rightarrow halo bias)
- density profile of the halo according to universal profile (NFW)
- concentration distribution as in Bullock et al. [2]

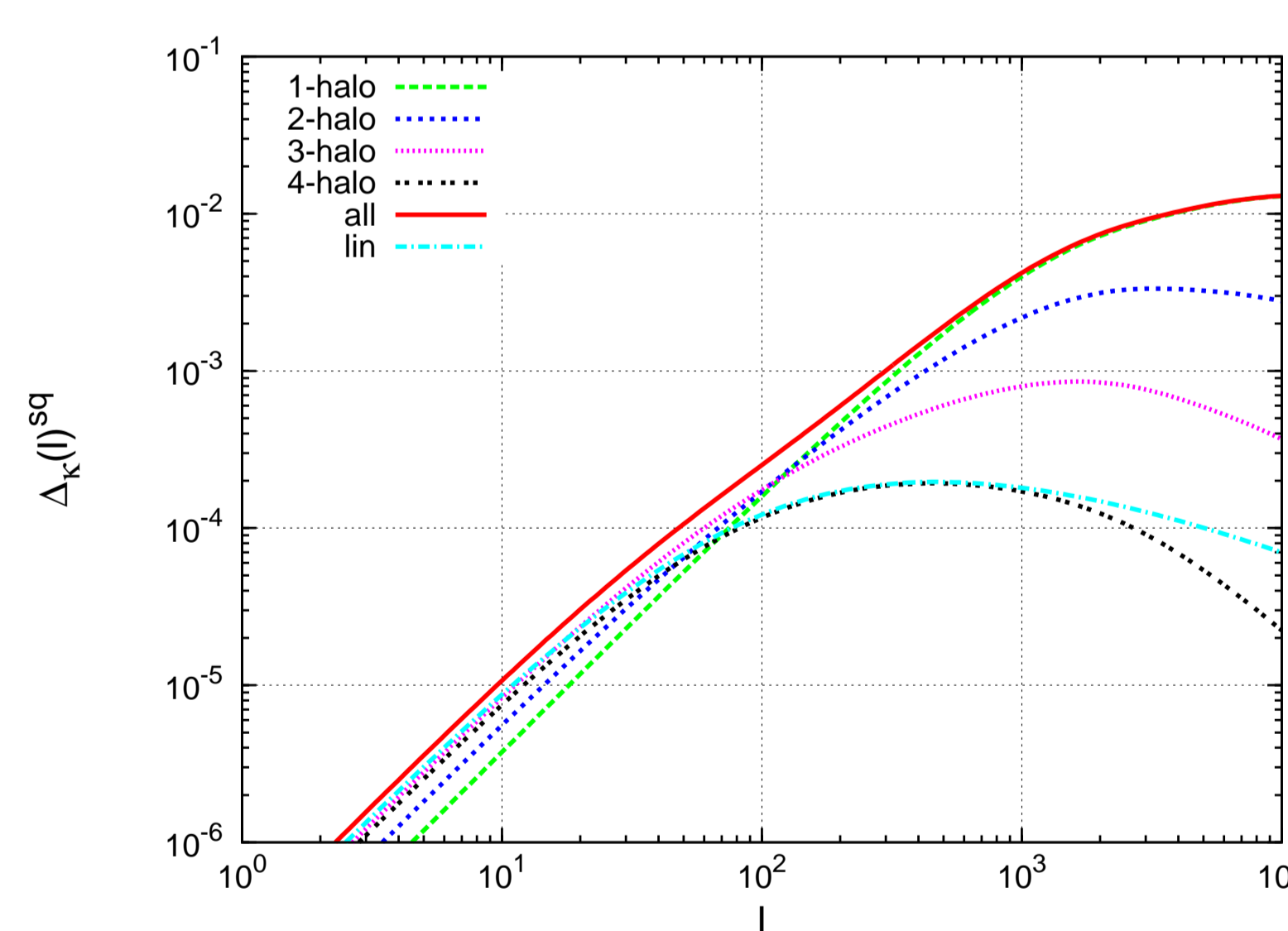


FIGURE 3: Convergence Trispectrum in the HM description. On small scales the 1-halo term dominates (green line).

Implementation:

- for the Halo Model we use our own implementation in C with the GSL-Library for numerical calculations and the ingredients as summarized above
- since the 1-halo term is dominant on small scales, we use the approximation $T_\kappa(l_i, l_j) \approx T_{1h}(l_i, l_j)$ in eq. (2) for analyzing the covariance matrix

Comparison with VIRGO-Simulations

For our work we use the N-body simulations of the VIRGO-collaboration published by Jenkins et al. (see [5]). The set of cosmological parameters used for the comparison with the halo model is:

Ω_m	Ω_Λ	h	Γ	σ_8	L_{box}/h^{-1} Mpc	N_{par}	m_{par}/M_\odot
0.30	0.70	0.7	0.21	0.9	141.3	256^3	1.4×10^{10}

From the simulations we use 200 realizations with a field view of $0.5^\circ \times 0.5^\circ$ and consider 30 bins of width $\Delta l \simeq 720$ starting at $l \simeq 720$.

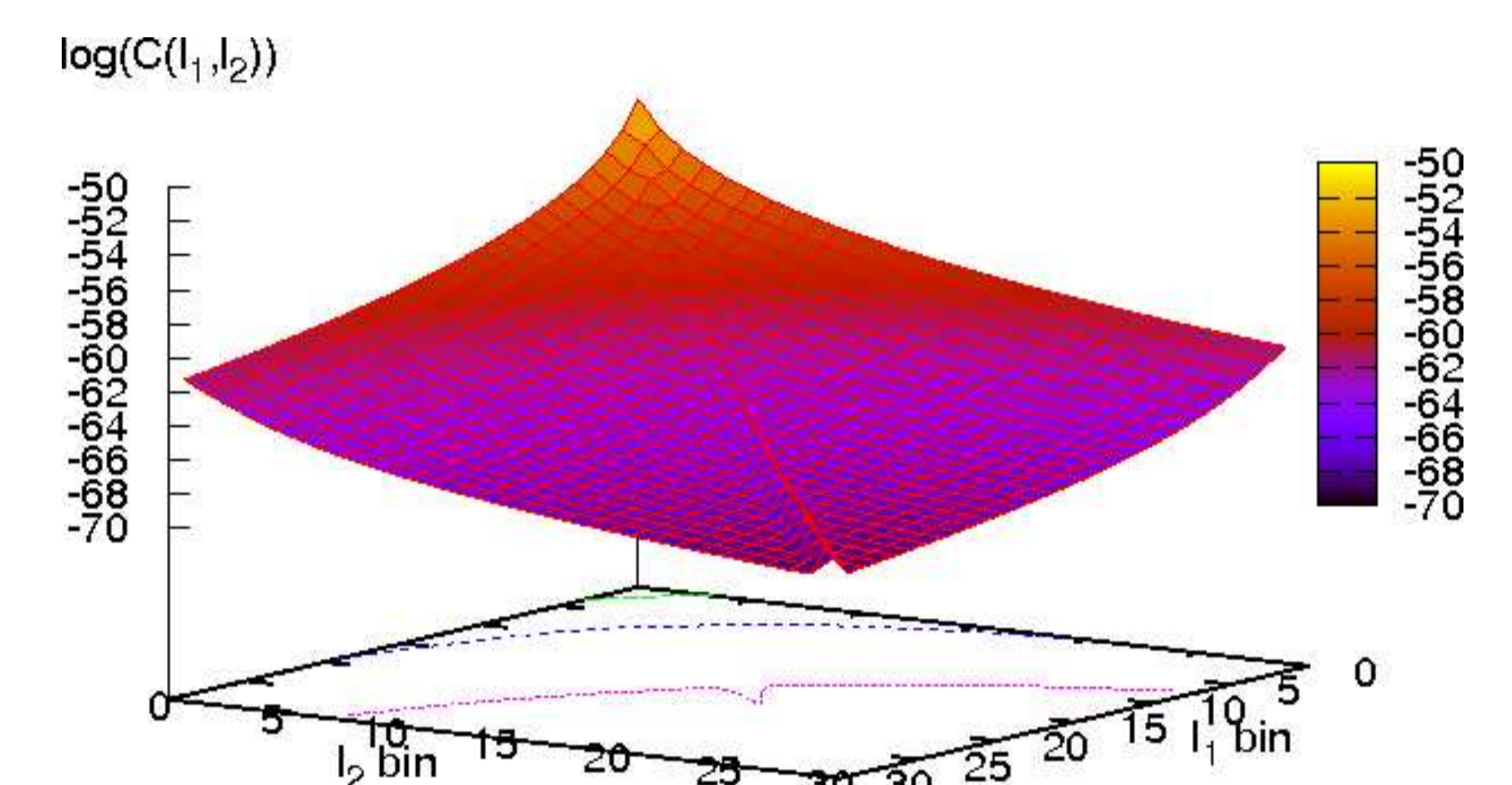


FIGURE 4: Covariance from the Halo Model with a Non-Gaussian contribution from the 1-halo term

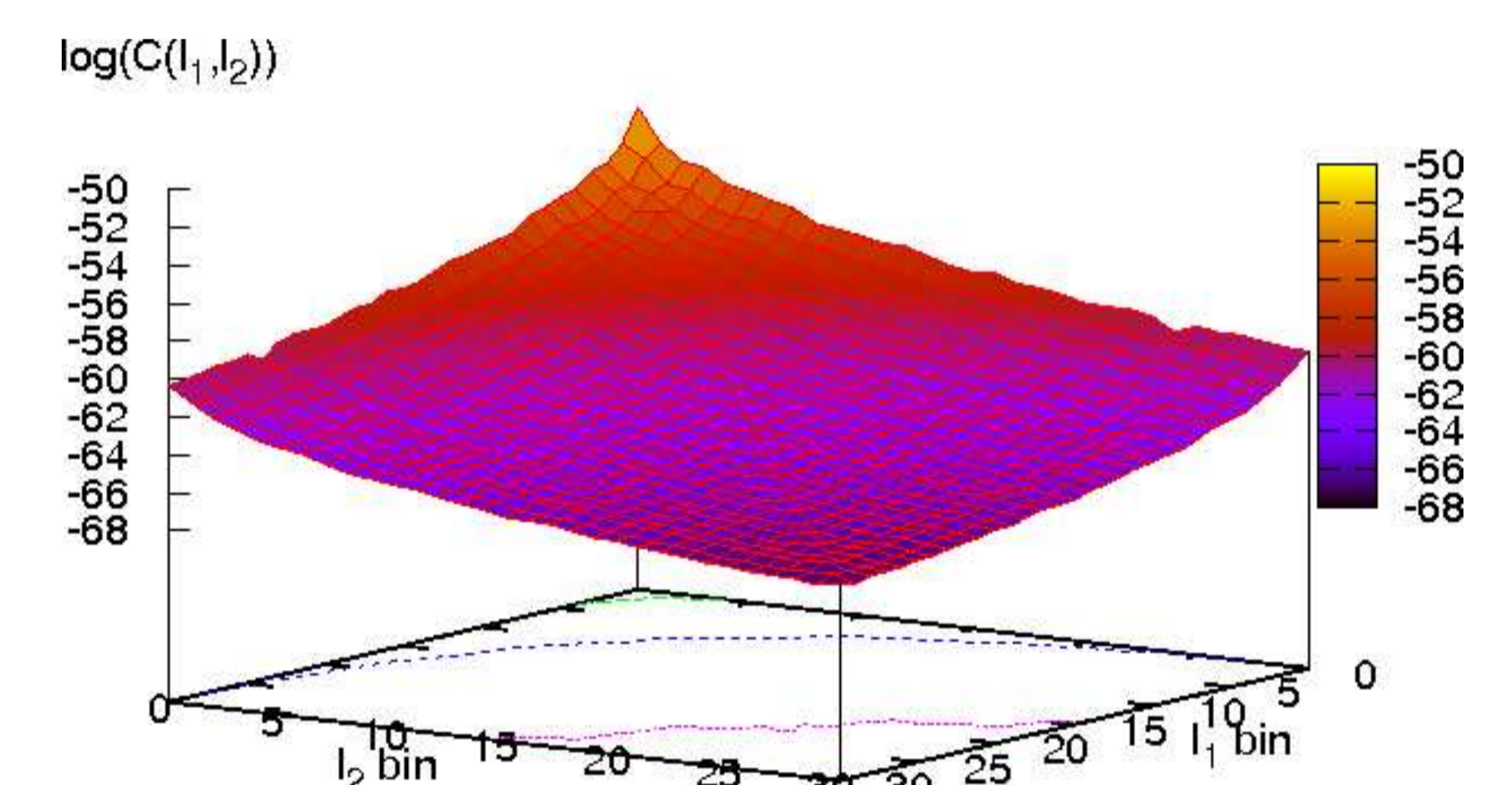


FIGURE 5: Covariance from the Virgo Simulation [5]

Preliminary Results and Outlook

- the HM reproduces the shape of the Virgo-simulations accurately
- on large scales the HM differs around 50% from the simulations
- on small scales both the HM description and the N-body simulation break down
- we plan to compare our model against N-body simulations for smaller bin width
- HM description of the trispectrum needs to be tested against simulations

References

- [1] Bartelmann, M. & Schneider, P. 2001, Phys. Rep., 340, 291
- [2] Bullock, J. S., Kolatt, T. S., Sigad, Y., et al. 2001, MNRAS, 321, 559
- [3] Cooray, A. & Hu, W. 2001, ApJ, 554, 56
- [4] Cooray, A. & Sheth, R. 2002, Phys. Rep., 372, 1
- [5] Jenkins, A., Frenk, C. S., Pearce, F. R., et al. 1998, ApJ, 499, 20
- [6] Soccimarro, R., Zaldarriaga, M., & Hui, L. 1999, ApJ, 527, 1